STM study of a rubrene monolayer on Bi(001): Structural modulations

Jun-Zhong Wang, Meng Lan, Ting-Na Shao, Guo-Qing Li, Yong Zhang, Cheng-Zhi Huang, Zu-Hong Xiong, Xu-Cun Ma, Jin-Feng Jia, and Qi-Kun Xue

Phys. Rev. B **83**, 235433 — Published 30 June 2011

DOI: 10.1103/PhysRevB.83.235433

STM study of rubrene monolayer on Bi(001): Structural modulations

Jun-Zhong Wang[1], Meng Lan[1], Ting-Na Shao[1], Guo-Qing Li[1], Yong Zhang[1], Cheng-Zhi Huang[1], Zu-Hong Xiong[1], Xu-Cun Ma[2], Jin-Feng Jia[3], and Qi-Kun Xue[3*]

[1] *School of Physical Science and Technology & MOE Key Laboratory on Luminescence and Real-Time Analysis, Southwest University, Chongqing 400715, China*

[2] *Institute of Physics, Chinese Academy of Science, Beijing 100190, China*

[3] *Department of Physics, Tsinghua University, Beijing 100084, China*

We report a structural modulation occurred in the rubrene monolayer grown on Bi(001) surface. A small sinusoidal variation of surface height plus the periodic distortion of molecular orientations have been observed by low temperature scanning tunneling microscopy. Further analyses demonstrate that this modulation results from the lattice rotation of rubrene monolayer with respect to Bi(001) substrate. Depending on the rotational direction of rubrene lattices, the modulation may exhibit either stripe ripples or zigzag patterns. The experimental data are discussed in term of mass density wave.

PACS numbers: 68.60.Bs; 68.35.Gy; 68.55.-a; 68.37.Ef ; 68.43.-h

* E-mail: qkxue@mail.tsinghua.edu.cn

I. Introduction

During the past decade, strain in physisorption and heteroepitaxy has attracted considerable interest.[1-4] Strain relief plays a central role in controlling the structure and morphology of epitaxial films. Understanding the mechanisms of strain relief may lead to better control of the growth process. Several strain relief mechanisms have been identified from heteroepitaxy, such as surface reconstruction,[5, 6] step bunching, [7, 8] faceting,[9] and formation of misfit dislocations.[10] For inert gas atoms physisorbed on graphite, Novaco and McTague predicted another mechanism of strain relief in term of mass density wave (MDW), which corresponds to a periodic small periodic variation in crystalline density.[11, 12] This structural modulation is subtle effect occurred in the incommensurate structures, where adorbate-adsorbate interaction dominates the lateral variation in adsorbate-substrate force.

For organic molecular system, it was also suggested that lattice mismatch between molecular layer and substrate results in the creation of MDW.[13-16] The most obvious difference is that, in the case of monatomic inert gas atoms, the spatial oscillation frequency of substrate potential is nearly equal to that of atomic adsorbates. As a result, MDW manifests itself as a periodic dislocation from the ideal lattice positions, as revealed by the diffraction experiments in Xe/Pt(111) system.[17-19] This is in contrast to the large organic molecular adsorbates with internal degrees of freedom, where the intermolecular spacing is substantially larger than the substrate lattice constants. Thus MDW in organic molecular layers may reveal some new features such as the periodic variations in the internal degree of freedom (molecular height, orientation, or lateral dimension).[15, 16]

In this paper, we report the direct observation of a structural modulation in rubrene ($C_{42}H_{28}$) monolayer with a low temperature scanning tunneling microscopy (LT-STM). The semi-metallic Bi(001) film was used as substrate to reduce the molecule-substrate interaction, owing to the very small density of states near Fermi level on Bi(001) surface.[20, 21] In addition to the height

oscillation, the modulation manifests a periodic variation in molecular orientations. Further analysis reveals that this modulation is a geometric effect. It is distinct from the usual Moiré pattern appeared in the incommensurate structures owing to the orbital overlaps in electronic states. Our observations could fit the criteria proposed by McTague and Novaco to define a MDW.

II. Experiments

The experiments were conducted in a Unisoku LT-STM system with the base pressure of 1.2 $\times 10^{-10}$ mbar. Bi (001) film was prepared by depositing 20 ML of Bi atoms on Si(111)-7×7 surface at room temperature (RT), with subsequent annealing at 120ºC. Rubrene molecules were deposited on Bi(001) film by vacuum sublimation from tantalum-cell with prior outgasing at 120ºC overnight. Through this paper we define the rubrene coverage in term of crystalline monolayer (ML) corresponding to the *a*-*b* plane of rubrene single crystals.

III. Results and discussion

A. Rubrene composite phase in submonolayer regime

In submonolayer regime (~0.7 ML), rubrene forms a composite phase consisting of rubrene crystalline domains and self-assembled domain walls [Fig. 1(a)]. The domain walls exhibit zigzag patterns with the individual segments aligned in $[\bar{1}\ \bar{1}\ 2]_{Bi}$ or $[\bar{2}\ 11]_{Bi}$ directions, respectively. From the close-up view [Fig. 1(b)], we observed the domain walls have a hexagonal lattice (c = 15.5 ± 0.1 Å), which is 2√3×2√3 reconstructed with respect to Bi(001). The rubrene crystalline domains have a rectangular lattice with a herringbone packing. The lattice constants are a = 12.6 ± 0.1 Å, and b = 7.3 ± 0.1 Å, similar to those of the *a*-*b* plane in rubrene single crystals (a_0 = 14.4 Å, b_0 = 7.2 Å).[22] According to the definition by Fenter *et al*., strain in organic film, δ, can be expressed as the fractional deviation of the unit cell aspect ratio from the bulk value.[23] Then $\delta = (a/b - a_0/b_0)/(a_0/b_0) = -13.7$ %, indicating a considerable large strain builds up in crystalline domains. This

large strain can be attributed to the small elastic constants of rubrene molecules associated with van der Waals interaction. By calculating the transformation matrix, we realized this crystalline domain is incommensurate with Bi(001) substrate. In addition, one of the two *c*-axes in domain walls is parallel to the *b*-axis of rubrene crystalline phase, while the *b*-axis and *a*-axis are parallel to $[\bar{1}01]_{Bi}$ and $[1\bar{2}1]_{Bi}$ directions, respectively.

The structural model for rubrene composite phase is shown in Fig. 1(d). Interestingly, we noticed that the *a* and *b* axes constitute a right-angle triangle with a 30 deg acute angle, which matches precisely with the underlying hexagonal lattice of Bi(001). This means that the orientation of rubrene lattice has been "locked in" by the symmetry axes of Bi(001) despite of the incommensurism. In fact, such lattice interlocking is similar to the Kurdjunov-Sachs (KS) orientational relationship in bcc(110)/fcc(111) system,[24, 25] where the diagonal of bcc(110) gets aligned with the bisector of angle between principal axes of fcc(111).

Further increasing the rubrene coverage leads to the growing of rubrene crystalline domains, and the onset of stripe ripple formation [Fig. 1(c)]. The lattice constants nearby the peak area become $a' = 13.8 \pm 0.1$ Å, and $b' = 7.3 \pm 0.1$ Å, corresponding to a strain $\delta' = -5.5$ %. It implies that 60 % of the previous strain in rubrene crystalline domains has been relaxed through the ripple formation. Most importantly, we found that the ripple reveals an evident lattice rotation (5 deg) relative to the lattice in crystalline domains.

B. Structural Modulation in rubrene monolayer

When the rubrene coverage increased to ~1 ML, all the domain walls change to rubrene crystalline domains. At the same time, large-scale array of surface ripples with nearly even spacing has been observed in the rubrene monolayer. Figure 2(a) shows a derivative of topographic STM image for rubrene monolayer, in order to enhance the surface feature of different terraces. The ripples exhibit linear stripe pattern with essentially parallel arrangement, similar to the wave fronts of plane waves. Fig. 2 (b) shows the close-up view of surface ripples,

which exhibit a small amplitude of ~0.5 Å and a period of ~8 nm in the *b*-axis direction [see the profile line in the upper panel of Fig. 2(d)]. The residual strain in stripe ripples changes to $\delta' = -6.1$ %. The insert is the atomic-resolution image of the underlying Bi substrate, which was obtained by applying a big pulse (~5 V) to the tip, to locally desorb rubrene molecules. After the pulse, a hole with diameter ~100 nm was opened in the rubrene monolayer due to the weak molecule-substrate binding. As a result, the bare Bi(001) surface was exposed at the bottom of hole. Examining the orientations of rubrene lattice, we noticed that the *b*-axis of rubrene unit cells is not aligned in the $[1\,\bar{2}\,1]_{Bi}$ direction anymore, whereas it rotates a counterclockwise angle (~5 deg), corresponding to the Novaco-McTague orientation epitaxy.[11, 12] Namely, the lattice interlocking occurred in rubrene composite phase has been now broken by orientational epitaxy.

Fig. 2(c) shows a STM image with sub-molecular resolution for the stripe ripples. Here we classify all the rubrene molecules in term of two non-equivalent molecular rows. In B-row there is only molecular height variation. In A-row, both height modulation and molecular orientation variation can be discerned. As demonstrated by the small arrows in A-row, there is a periodic variation in the direction of molecular axis, as the position moving from trough to peak. The lower panel of Fig. 2(d) shows a plot of the angle between molecular axis and the *a*-axis of rubrene unit cells as a function of molecular position.

It should be emphasized that the stripe ripples formation is a geometric effect owing to the variation of molecular internal degrees of freedom. As revealed by the bias-independent STM images in Fig. 3, the stripe ripples do not vary with the scanning bias, although the protrusions of individual rubrene molecules exhibit some weak modifications. This structural modulation is distinct from the usual Moiré pattern appeared in the incommensurate overlayer, which reflects a spatial modulation of tunneling current due to superposition of density of states between overlayer and substrate.[26] Thus the Moiré patterns might be invisible at certain sample bias.

C. Zigzag ripples after annealing

When the rubrene monolayer is annealed to ~100°C, some stripe ripples change to zigzag ones [Fig. 4(a)]. The segments of surface ripples are aligned along two directions separated by ~120 deg angle. More interestingly, we found that the neighboring zigzag ripples constitute a head-to-head configuration, leading to an ordered rhombus-like array, Fig. 4(b). It means that there exist strong attractive interactions between the "joints" of adjacent zigzag ripples. From the close-up view in Fig. 4(c), it is found that for the two adjacent ripples with different orientations, their *b*-axes exhibit opposite rotations (± 4.5 deg) with respect to $[2\,\bar{1}\,\bar{1}]_{Bi}$ direction, but the *a*-axis is still in the $[0\,\bar{1}\,1]_{Bi}$ direction. We speculate that there might be a slight energy difference between the two opposite lattice rotations of rubrene monolayer. At RT or low temperature, the lattice rotation toward one direction may be more energetically favored than the other, leading to the parallel stripe ripples. On the other hand, at elevated temperature, the slight energy difference between the two lattice rotations has been smeared out by thermal fluctuation, leading to the two possible lattice rotations occurred simultaneously. It is the competition between the two opposite lattice rotations results in the zigzag pattern of structural modulation in rubrene monolayer.

D. Discussion

Based on the experimental observations, we noticed that the structural modulation in rubrene monolayer resembles the predicted MDW features in organic molecular layers proposed by Forrest.[15-16] In rubrene monolayer we have observed a number of stripe ripple arrays with different periods and orientations. Thus the distribution of stripe ripples is non-homogenous over the sample surface. By statistically analyzing the experimental data, we found a general tendency that the period of stripe ripples decreases and the lattice rotation angle increases with increasing lattice misfit. This is qualitatively consistent with the theoretical calculation based on MDW model,[18] which describes the MDW periodicity in term of *Q*:

$$Q \cong (8\pi / d)(m / \sqrt{3})(1 + m / 8) \qquad (1)$$

where *Q* is the MDW wave-vector, *d* the lattice constant of adsorbates, and *m* the lattice misfit.

For very small lattice misfit ($m \to 0$), the substrate-molecule interaction will dominate the intermolecular interaction. Equation (1) would lead to a MDW with very large period, indicating a rather weak modulation of MDW. On the other hand, for large lattice misfit ($m \to \infty$), the intermolecular interaction is stronger than the substrate-molecule interaction. Equation (1) would result in a very small period of MDW, which means the modulation of MDW is very strong.

The quantitative comparison between the observed modulation and theoretical model of MDW is displayed in Fig. 5. Fig. 5(a) shows the variation of stripe ripple periods with lattice misfit. For larger misfits, the experimental data is consistent with theoretical prediction, while for smaller misfits, the measured periods are smaller remarkably than the calculated ones. In Fig. 5(b), we plot the dependence of overall lattice rotation angle $(\theta_a + \theta_b)/2$ on lattice misfit, since the rotation of *a*-axis is slightly out of step with that of *b*-axis in rubrene unit cell. The red solid line is theoretical result based on Gordon's analysis: $\vartheta \approx m/\sqrt{3}$. A qualitative agreement can be derived, but the observed rotation angle is larger than the theoretical predication. The discrepancies between the experimental observation and MDW's model can be attributed to the fact that, Gordon's analysis is based on the linear response treatment of the adsorbate-substrate interaction, which is justified for large misfit, whereas the lattice misfit in rubrene monolayer is rather small (0~10 %).

IV. Conclusion

In summary, a structural modulation has been observed in the rubrene monolayer grown on Bi(001) with LT-STM. The modulation reveals not only a sinusoidal variation in surface height, but also a periodic distortion in molecular orientations. Meanwhile, a molecular lattice rotation relative to Bi(001) substrate has been identified. Depending on the rotational direction of rubrene lattices, the modulation may exhibit either stripe ripples or zigzag patterns. For large lattice misfits, the ripple's period is quantitatively in agreement with theoretical model of MDW. These findings provide essential information and a new insight into the strain relaxation mechanism in

organic molecular layers.

References

1. L. W. Brush, R. D. Diehl, and J. A. Venable, Rev. Mod. Phys. **79**, 1381 (2007).
2. M. Gsell, P. Jakob, and D. Menzel, Science **280**, 717 (1998).
3. H. Brune, M. Giovannini, K. Bromann, and K. Kern, Nature **394**, 451 (1998).
4. K. Thurmer, R. Q. Hwang, and N. C. Bartelt, Science **311**, 1272 (2006).
5. Y.-W. Mo and M. G. Lagally, J. Cryst. Growth **111**, 876 (1991).
6. R. Butz and S. Kampers, Appl. Phys. Lett. **61**, 1307 (1992).
7. J. Tersoff, Y. H. Phang, Z. Zhang, and M. G. Lagally, Phys. Rev. Lett. **75**, 2730 (1995).
8. F. Liu, J. Tersoff, and M. G. Lagally, Phys. Rev. Lett. **80**, 1268 (1998).
9. Y.-W. Mo, D. E. Savage, B. S. Swartzentruber, and M. G. Lagally, Phys. Rev. Lett. **65**, 1020 (1990).
10. J. W. Matthews, and E. A. Blakeslee, J. Cryst. Growth. **27**, 118 (1974).
11. A. D. Novaco and J. P. McTague, Phys. Rev. Lett. **38**, 1286 (1977).
12. J. P. McTague and A. D. Novaco, Phys. Rev. B **19**, 5299 (1979).
13. Y. Zhang and S. R. Forrest, Phys. Rev. Lett. **71**, 2765 (1993).
14. S. R. Forrest and Y. Zhang, Phys. Rev. B **49**, 11297 (1994).
15. S. R. Forrest and P. E. Burrows, Supramolecular Science **4**, 127 (1996).
16. S. R. Forrest, Chem. Rev. **97**, 1793 (1997).
17. K. Kern, R. David, R. L. Plamer, and G. Comsa, Phys. Rev. Lett. **56**, 2823 (1986).
18. M. B. Gordon, Phys. Rev. Lett. **57**, 2094 (1986).
19. K. Kern, P. Zeppenfeld, R. David, and G. Comsa, J. Vac. Sci. Technol. A **6**, 639 (1988).
20. G. E. Thayer, J. T. Sadowski, F. M. z. Heringdorf, T. Sakurai, and R. M. Tromp, Phys. Rev. Lett. **95**, 256106 (2005).
21. H. Kakuta, T. Hirahara, I. Matsuda, T. Nagao, S. Hasegawa, N. Ueno, and K. Sakamoto, Phys. Rev. Lett. **98**, 247601 (2007).
22. D. E. Henn, W. G. Williams, and D. J. Gibbson, J. Appl. Cryst. **4**, 256 (1971).
23. P. Fenter, F. Schreiber, L. Zhou, P. Eisenberger, and S. R. Forrest, Phys. Rev. B. **56**, 3046 (1997).
24. A. Zangwill, Physics at Surface (Cambridge University Press, Cambridge, 1988), pp. 422.
25. E. Bauer and J. H. v. d. Merwe, Phys. Rev. B **33**, 3657 (1986).
26. D. E. Hooks, T. Fritz, and M. D. Ward, Adv. Mater. **13**, 227 (2001).

Acknowledgement

This work was supported by the National Natural Science Foundation of China (Grant No. 10974156, 10974157, 21035005), and Natural Science Foundation Project of CQ CSTC (Grant No. 2008BB4003).

Figure Captions

Fig. 1. (color online). STM images of the rubrene composite phase. (a) rubrene crystalline domains separated by zigzag domain walls, 3.0 V. (b) Close-up view of the rubrene composite phase, 2.5 V. (c) Onset of a surface ripple formation in rubrene composite phase, 2.5 V. (d) Schematic model of rubrene composite phases with respect to Bi(001).

Fig. 2. (color online). Structural modulation appeared in the rubrene monolayer. (a) Derivative of a topographic STM image for the stripe ripples appeared in rubrene monolayer, 3.8 V. (b) Close-up view of the stripe ripples, 4.5 V. Insert is the atomic-resolution STM image of the underlying Bi substrate. The red arrow indicates the $[1\,\bar{2}\,1]$ direction of Bi substrate. (c) Periodic distortions in molecular orientation and lateral dimension appeared in stripe ripples, -2.5 V. (d) Upper: line profile along the red dotted line in (b); Lower: a plot of the angle ϕ between the molecular axis and *a*-axis of unit cell, as a function of molecule position, where the solid line is a Gaussian fit.

Fig. 3. (color online). Bias independent STM images of the stripe pattern of structural modulation. The sample bias varies from (a) +2.5 V, (b) +1.5 V, (c) +1.0 V, (d) -1.5 V, (e) -2.5 V, and to (f) -3.5 V, 15 nm $\times$ 15 nm.

Fig. 4. (color online). Zigzag ripples appeared in the annealed rubrene monolayer. (a) Coexistence of the zigzag and stripe ripples, -4.5 V. (b) Head-to-head configuration of the adjacent zigzag ripples, 4.5 V. (c) Close-up view of zigzag ripples, 4.5 V.

Fig. 5. (color online). Comparison between the observed structural modulation and theoretical model of MDW. (a) Plot of stripe ripple periods as a function of lattice misfit. (b) Plot of the overall lattice rotation angle in rubrene monolayer, $(\varphi_a+\varphi_b)/2$, as a function of lattice misfit. The black lines are the fitting of experimental data, while the red lines in (a) and (b) show the MDW's periods and the calculated lattice rotation based on Gordon' analysis.

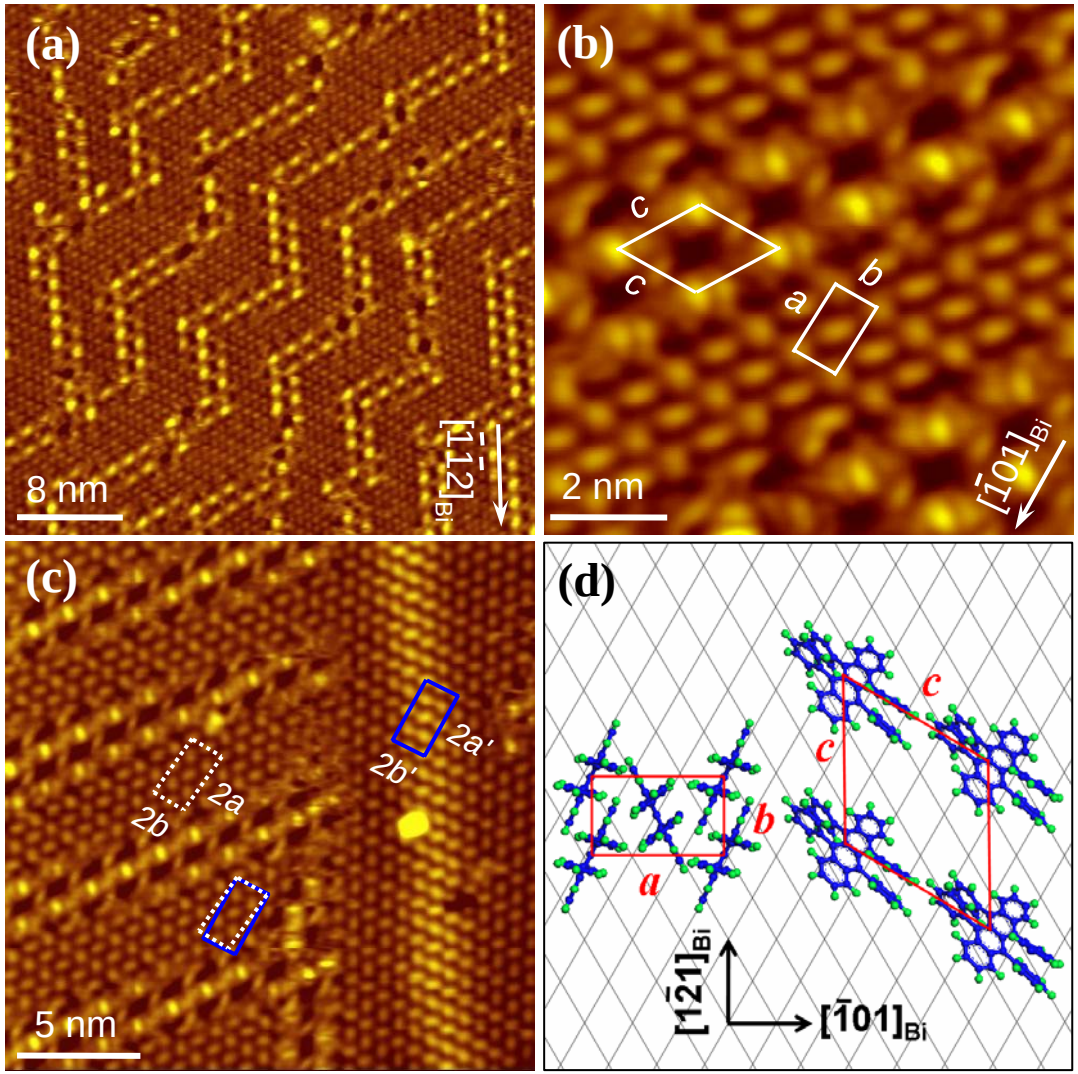

Wang *et al.*, Figure 1

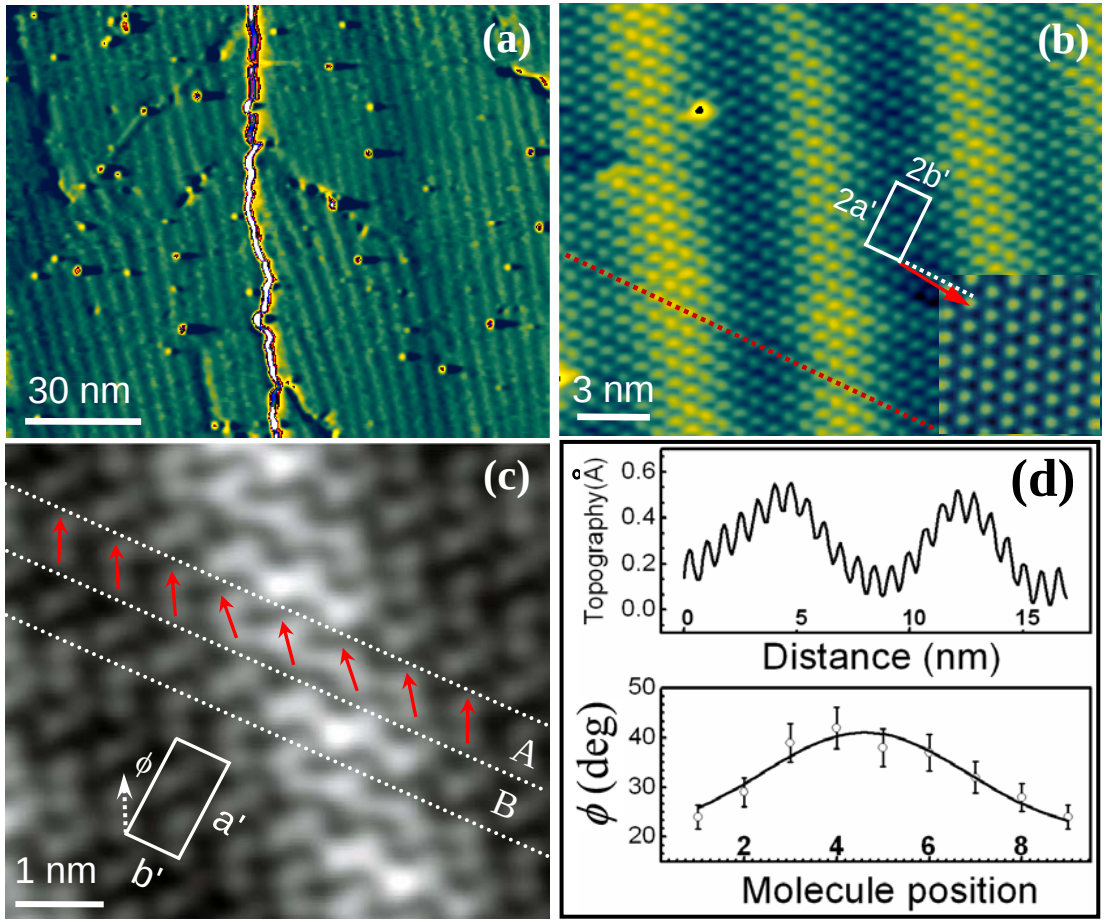

Wang *et al.*, Figure 2

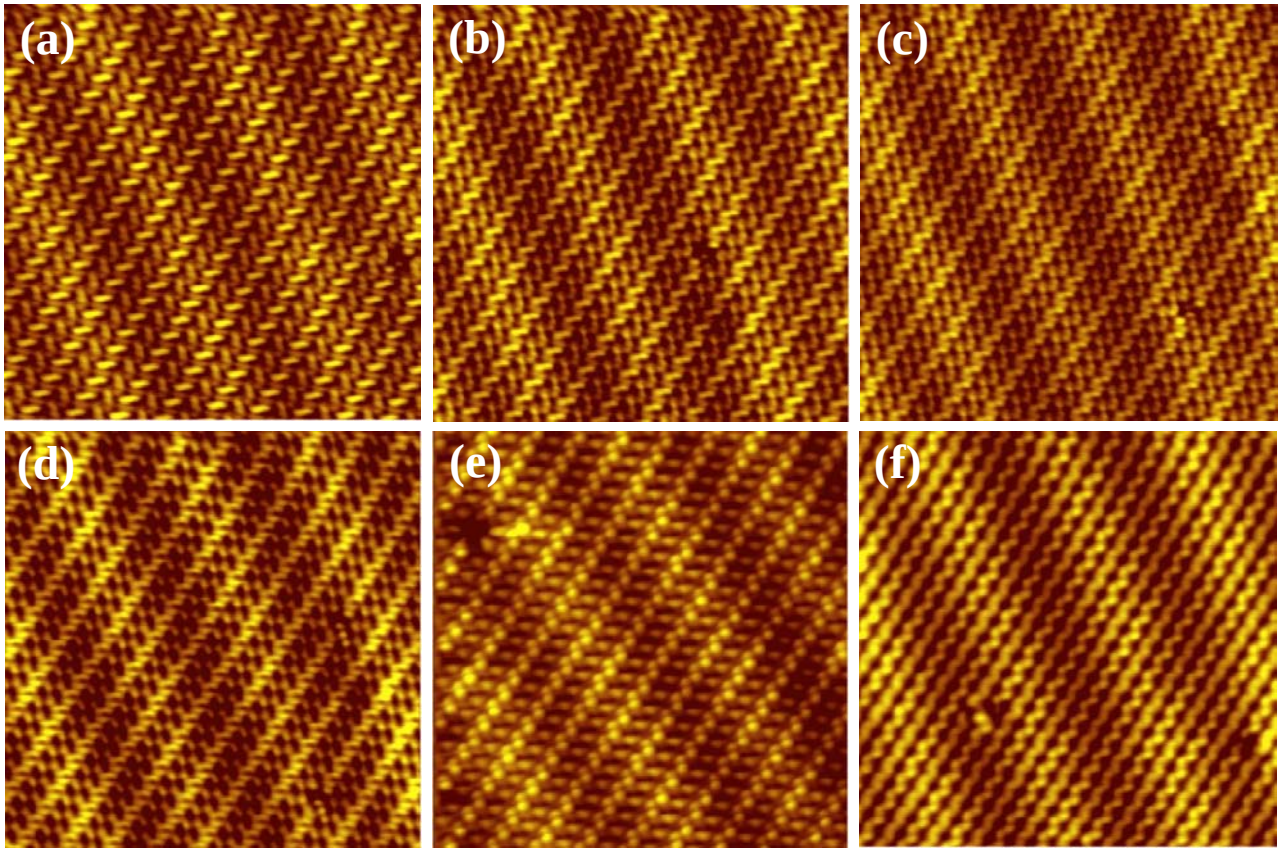

Wang *et al.*, Figure 3

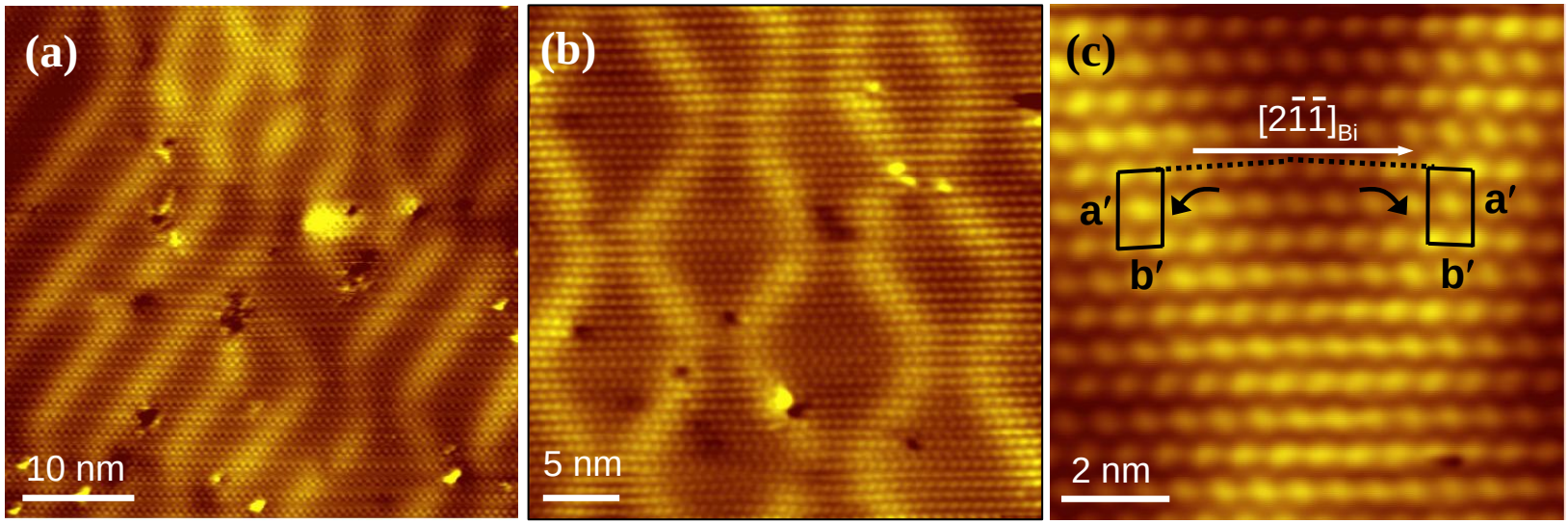

Wang *et al.*, Figure 4

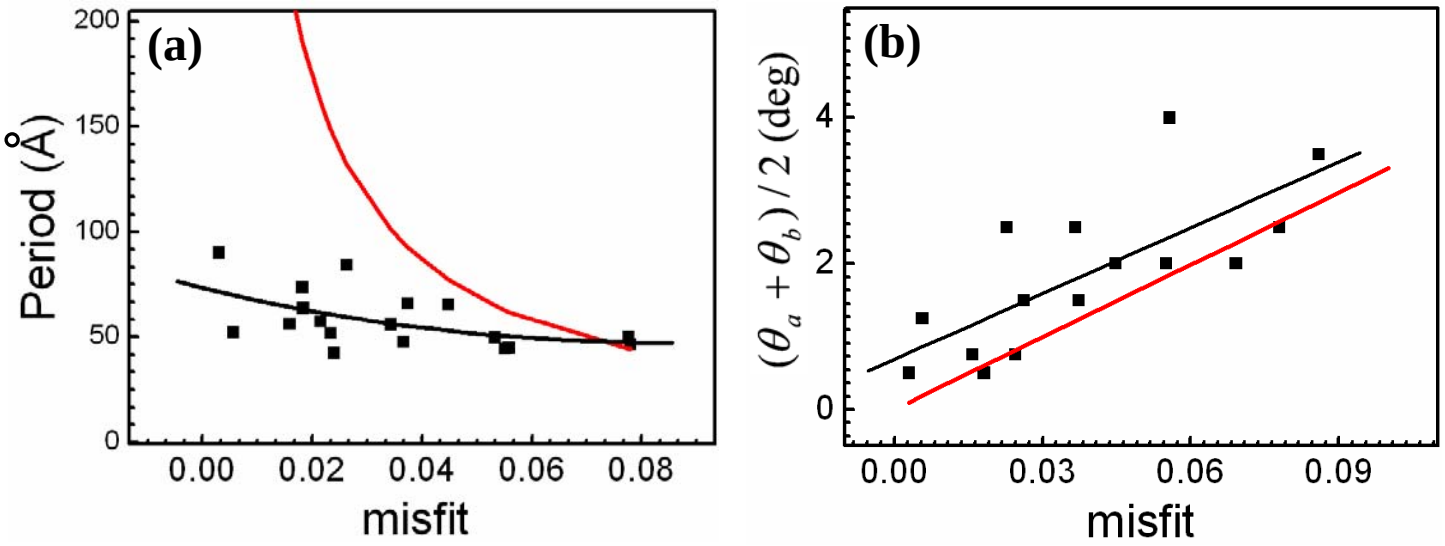
(a)
Period (Å)
200
150
100
50
0
0.00
0.02
0.04
0.06
0.08
misfit
(b)
$(\theta_a + \theta_b) / 2$ (deg)
4
2
0
0.00
0.03
0.06
0.09
misfit